INSTITUTE OF PHYSICS PUBLISHING JOURNAL OF PHYSICS B: ATOMIC, MOLECULAR AND OPTICAL PHYSICS

J. Phys. B: At. Mol. Opt. Phys. **37** (2004) 4221–4237 PII: S0953-4075(04)84895-8

# Time-delay matrix analysis of resonances: application to the positronium negative ion

**Akinori Igarashi**[1] **and Isao Shimamura**[2]

[1] Department of Applied Physics, Miyazaki University, Miyazaki 889-2192, Japan
[2] The Institute of Physical and Chemical Research (RIKEN), Wako, Saitama 351-0198, Japan

E-mail: igarashi@phys.miyazaki-u.ac.jp

Received 12 August 2004
Published 26 October 2004
Online at stacks.iop.org/JPhysB/37/4221
doi:10.1088/0953-4075/37/21/001

**Abstract**

A procedure to analyse resonances in scattering and photoionization calculations is discussed. It is theoretically connected to a general relation between the trace of the time-delay matrix and the energy derivative of the eigenphase sum. This procedure is especially useful in analysing resonances with strong background contributions, such as shape resonances lying just above the threshold of a new channel with an overcritical dipole field. In this case the background eigenphase sum diverges towards the threshold, and it can easily change the time delay due to an $S$-matrix pole into a negative time delay, or time advance. As an application, we analyse results of hyperspherical close-coupling calculations of S-, P-, D-, F-, G- and H-wave resonances in the positronium negative ion $Ps^-$ near the $Ps(n = 2, 3)$ thresholds. We find examples of a strong background leading to an overall time advance and the dipole oscillation in the cross section above and near a threshold.

## 1. Introduction

Resonance analysis of atomic and molecular scattering and photoionization calculations has often been based on the Breit–Wigner (BW) formulae [1] for the phase shift and for the $S$ matrix. For multichannel problems, the BW one-level formula for the $S$ matrix can be shown to lead to exactly the same form for the eigenphase sum as the BW formula for the single-channel phase shift [2]. This has been exploited in the fitting to the eigenphase sum, obtained from continuum-state calculations, to extract resonance parameters, namely, resonance positions and widths.

Later, it was realized that the derivative of the eigenphase sum $\delta(E)$ with respect to the energy $E$ is more useful than the eigenphase sum itself for the purpose of resonance analysis [3]. This has both practical and physical aspects. For one thing, resonances stand out more

  

clearly in the derivative $\mathrm{d}\delta(E)/\mathrm{d}E$ than in the eigenphase sum itself. For another, the derivative $\mathrm{d}\delta(E)/\mathrm{d}E$ is related to the lifetime of the resonance state, which allows transparent physical interpretation. More specifically, $\mathrm{d}\delta(E)/\mathrm{d}E$ can be proved to be proportional to both the trace (or the diagonal sum) and the largest eigenvalue $q_{\max}$ of the lifetime or delay-time matrix $Q(E)$, defined by Smith [4], if one assumes the BW formula for the $S$ matrix with a *constant* background $S$ matrix independent of the energy [5]. Both $q_{\max}$ and the trace (Tr $Q$) of the $Q$ matrix have a Lorentzian profile in the resonance energy region. The largest eigenvalue, studied numerically by Burke *et al* [6], for example, has often been paid particular and more attention than Tr $Q(E)$ in resonance analysis [7].

On the other hand, results of $R$-matrix method calculations were analysed recently by taking advantage of the known analytic forms of the $R$ matrix and associated matrices when differentiating with respect to the energy [8–10] to find out the maximum of the Lorentzian form. This method was found useful for automatic and fast analysis of the results of $R$-matrix method calculations.

When the resonance is narrow or when the background $S$ matrix depends only weakly on the energy, the resonance analysis is fairly simple, the results depending little on the choice of the analysis procedure among the ones mentioned so far. Indeed, the pure Lorentzian form of $\mathrm{d}\delta(E)/\mathrm{d}E$ reduces to a simple expression for the resonance position and width [8–11]. However, there are cases where the energy dependence of the background $S$ matrix is far from negligible and plays a significant role. For dealing with such cases, the background contribution was assumed to be made by the tail of another resonance in [8–10]. This effectively means to deal with overlapping resonances with no background contributions. Then Tr $Q(E)$ can be proved in a straightforward manner to be still proportional to $\mathrm{d}\delta(E)/\mathrm{d}E$, which allows the same kind of physical interpretation of the derivative as in the case of an isolated resonance with a constant background.

However, mechanisms other than the tail of an adjacent resonance can make a background contribution having various forms of energy dependence. In fact, the same proportionality relation Tr $Q(E) \propto \mathrm{d}\delta(E)/\mathrm{d}E$ can be proved for *any* form of the energy dependence of $\delta(E)$ or $Q(E)$, i.e. both off resonance and on resonance with any background contribution; see the appendix in [12]. This relation attaches physical significance to resonance analysis of $\mathrm{d}\delta(E)/\mathrm{d}E$ in general in the form of the pure Lorentzian profile augmented by the derivative of the background eigenphase sum of any form, including the cases of very broad resonances and of strong threshold effects. This will be discussed in the next section. Incidentally, the energy dependence of the largest eigenvalue of the $Q$ matrix is theoretically still unknown for the case of background $S$ matrix of general energy dependence.

As an application of this theory, the nonrelativistic Coulomb three-body system $e^+e^-e^-$ (or the positronium negative ion $Ps^-$), or equivalently, $e^+e^-e^+$ (or $Ps^+$), will be treated in this paper. This system is equivalent to other similar systems, such as the muonic systems $\mu^+\mu^-\mu^\pm$, mesonic systems $K^+K^-K^\pm$ and the proton–antiproton system $pp\overline{p}$, if the energy is scaled by the particle mass, to the extent that the interactions other than the nonrelativistic Coulomb interactions are neglected. In terms of the mass ratio between the two equal particles and the third particle, the system $Ps^-$ lies intermediate between the negative ion $H^-$ (atomic limit) and the molecular ion $H_2^+$ (molecular limit), although $Ps^-$ is more similar to $H^-$ than to $H_2^+$.

There is only one bound state in $Ps^-$, which was produced experimentally by Mills [13]. Its annihilation rate was also measured subsequently [14]. An improved measurement of the annihilation rate is currently being prepared [15]. Also, a recent experimental proposal on photon-impact electron detachment, or photodetachment, from $Ps^-$ is worth noting [16]. The bound state of $Ps^-$ was calculated elaborately by many authors [17–20], and the calculations

were extended to resonance states. The complex-coordinate rotation method, which avoids scattering calculations and tries to obtain poles of the $S$ matrix in the complex-energy plane, was applied extensively to $Ps^-$ resonances up to the threshold for the formation of $Ps(n = 5)$ for the total angular momentum $L \leqslant 8$, and up to the $Ps(n = 7)$ threshold for $L \leqslant 2$ [21–28]. The $Ps^-$ resonance calculations by other methods are relatively fragmentary. Some are based on the hyperspherical coordinates; Botero and Greene [29] used an adiabatic treatment to investigate resonances lying near the $Ps(n = 2)$ threshold. The close-coupling method in terms of the hyperspherical coordinates was applied by Zhou and Lin [30] to S-wave resonances and by Igarashi *et al* [31] to $^1P^o$ resonances in relation to the photodetachment of $Ps^-$. Toyota and Watanabe [32] applied a Siegert pseudostate method in terms of the hyperspherical elliptic coordinates to $^1S$ resonances and antiresonances. For other theoretical studies, see [28, 33, 34] and references cited therein.

In the present work, we extend our previous hyperspherical close-coupling calculations to resonances in the partial waves $0 \leqslant L \leqslant 5$ and associated with the $Ps(n = 2)$ and $Ps(n = 3)$ thresholds. The theory of the next section is applied for the determination of resonance parameters. The cross sections for electron scattering by Ps(1s) are also reported near the $Ps(n = 2)$ threshold, where a rich resonance structure is clearly seen.

## 2. Time-delay matrix analysis

In search of resonances, multichannel continuum-state calculations are carried out for varying total energy $E$. The asymptotic boundary condition may be either that for the scattering wavefunction or that for the final state of photoionization/photodetachment. The $S$ matrix and the eigenphase sum $\delta(E)$ are common to both boundary conditions. For $E$ near the position $E_r$ of an isolated resonance, $\delta(E)$ is considered to follow the Breit–Wigner one-level formula

$$\delta(E) = \delta^0(E) + \arctan\left(\frac{\Gamma/2}{E_r - E}\right) \tag{1}$$

approximately, where $\Gamma$ is the total resonance width [2]. If the background eigenphase sum $\delta^0(E)$ is almost constant, $\delta(E)$ increases by $\pi/2$ between $E = E_r - \Gamma/2$ and $E_r + \Gamma/2$, and nearly by $\pi$ in a region of a width of several multiples of $\Gamma$.

Equation (1) may be fitted to the eigenphase sum $\delta(E)$ obtained from multichannel continuum calculations. Thus the resonance parameters $E_r$ and $\Gamma$ are determined. In this fit, the slowly varying background eigenphase sum may be represented by a polynomial such as

$$\delta^0(E) = C_0 + C_1 E + C_2 E^2, \tag{2}$$

where $C_i$ ($i = 0, 1, 2$) are fitting parameters, although the quadratic term may often be negligible. This procedure suffices for most resonances lying far above the threshold of the opening of any new channel.

In a channel separating into a charged particle and a hydrogenlike atom, an asymptotic dipole potential $\hbar^2\alpha/(2MR^2)$ (including the centrifugal potential) can appear at large distances $R$ between the two subsystems, $M$ being the reduced mass between them [35]. This occurs because of the linear Stark effect due to degenerate sublevels of the hydrogenlike atom. If this dipole potential is overcritically attractive, namely, if $\alpha < -1/4$, then the eigenphase sum includes a term $\delta^0_{\rm dip}(E)$ that diverges logarithmically close to the threshold $E_{\rm th}$ for these sublevels [35–37], $\delta^0_{\rm dip}(E)$ satisfying a formula

$$\tan\delta^0_{\rm dip}(E) = -\coth(\pi\nu)\tan\{\nu\ln(E - E_{\rm th}) + \chi\}, \qquad \nu \equiv \frac{(-1 - 4\alpha)^{1/2}}{4} \tag{3}$$

with an almost constant $\chi$ for $E \simeq E_{\rm th}$.

This formula reduces to a simple relation $\delta^0_{\rm dip}(E) \simeq -\nu \ln(E - E_{\rm th}) - \chi$ for large $|\alpha|$, but (3) is awkward in actual applications to a fitting procedure, in general. Instead, we have found, perhaps for the first time, that an expression

$$\delta^0(E) = -C_{-1} \ln(E - E_{\rm th}) + C_0 + C_1 E + C_2 E^2, \tag{4}$$

or even without the last term, is convenient and useful for practical purposes of resonance fitting just above a threshold that produces an overcritical dipole potential. This form should be more reasonable than the one used in [38], which includes a term inversely proportional to $E - E_{\rm th}$. Indeed, we have found that (4) gives a better fit than the procedure of [38]. As the energy increases farther and farther from $E_{\rm th}$, the logarithmic term becomes more and more slowly varying with the energy, thus making a simpler form (2) accurate enough.

An alternative, more useful fitting method is based on the lifetime matrix $Q(E)$ defined by Smith [4] and often called the time-delay matrix in the later literature. This matrix is related to the $S$ matrix by

$$Q(E) = \mathrm{i}\hbar S \frac{\mathrm{d}S^\dagger}{\mathrm{d}E} = -\mathrm{i}\hbar \frac{\mathrm{d}S}{\mathrm{d}E} S^\dagger = Q^\dagger(E). \tag{5}$$

Any diagonal element $Q_{ii}(E)$ of $Q(E)$ is real and has a significance of the average delay time in scattering starting from the initial channel $i$. In a similar way, any eigenvalue $q_\alpha(E)$ of $Q(E)$ may be interpreted as the average delay time in scattering starting from the artificial initial channel $\alpha$ formed by that linear combination of the physical channels $i$ that is defined in terms of the corresponding eigenvector $\mathbf{c}_\alpha(E)$.

Smith [4] conjectured that a large eigenvalue of the $Q$ matrix should be identified with the exponential decay time of a long-lived metastable state represented by the corresponding eigenvector. Later, an illuminating result was obtained [5] on the assumption of the Breit–Wigner one-level formula [1]

$$S_{ij} = \exp\{\mathrm{i}(\phi_i + \phi_j)\} \left( \delta_{ij} - \frac{\mathrm{i}\Gamma_i^{1/2}\Gamma_j^{1/2}}{E - E_{\rm r} + \mathrm{i}\Gamma/2} \right), \qquad \Gamma \equiv \sum_i \Gamma_i \tag{6}$$

for $S$ matrix elements with constant background phases $\phi_i$ and $\phi_j$, and constant partial widths $\Gamma_i$ and $\Gamma_j$; only one of the eigenvalues, say $q_1(E)$, of the $Q$ matrix is different from zero, and it shows the Lorentzian profile

$$q_1(E) = \sum_\alpha q_\alpha(E) = \mathrm{Tr}\, Q(E) = \frac{\hbar\Gamma}{(E - E_{\rm r})^2 + (\Gamma/2)^2}. \tag{7}$$

Each diagonal element $Q_{ii}(E)$ is equal to $\mathrm{Tr}\, Q(E)$ multiplied by a factor $\Gamma_i/\Gamma$. Equation (7) is exactly the derivative of (1) times $2\hbar$ if the background eigenphase sum $\delta^0$ is independent of the energy $E$. Smith [4] had derived this Lorentzian form for the single-channel $Q(E)$ in a resonance region.

Such a Lorentzian peak would stand out more conspicuously against the background than the increase in the eigenphase sum. In the light of (7), therefore, either the largest eigenvalue $q_{\rm max}(E)$ of $Q(E)$ [7] or $\mathrm{Tr}\, Q(E)$ (or $2\hbar \mathrm{d}\delta/\mathrm{d}E$) [8–10] may be used to locate resonances and to fit (7) to calculated data for the determination of the resonance parameters. At this stage, no preference between the use of $q_{\rm max}(E)$ and of $\mathrm{Tr}\, Q(E)$ to the other seems to be supported theoretically.

For proving the relation

$$\mathrm{Tr}\, Q(E) = 2\hbar \frac{\mathrm{d}\delta(E)}{\mathrm{d}E}, \tag{8}$$

the assumption of the Breit–Wigner formula with a constant background is unnecessary. In fact, this general theorem was proved for *any functional form* of $\delta(E)$ or $\mathrm{Tr}\, Q(E)$, that is,

by assuming no particular form of the interaction or even the kind of the process. The only necessary assumptions were that the matrices $S(E)$ and $dS/dE$ exist and that $Q(E)$ be written as (5) (see [12]). Because equation (8) was proved for arbitrary $\delta(E)$, a resonance formula

$$\mathrm{Tr}\, Q(E) = \frac{\hbar\Gamma}{(E - E_\mathrm{r})^2 + (\Gamma/2)^2} + 2\hbar\frac{\mathrm{d}\delta^0(E)}{\mathrm{d}E} \tag{9}$$

follows from (1) for the background eigenphase sum $\delta^0(E)$ of any energy dependence. A both practically and physically reasonable fitting formula follows from (4) as

$$\frac{\mathrm{d}\delta}{\mathrm{d}E} = \frac{\Gamma/2}{(E - E_\mathrm{r})^2 + (\Gamma/2)^2} - \frac{C_{-1}}{E - E_\mathrm{th}} + C_1 + 2C_2E \tag{10}$$

just above a threshold $E_\mathrm{th}$ associated with an overcritical dipole potential, the term inversely proportional to $E - E_\mathrm{th}$ being unnecessary otherwise. The last term, $2C_2E$, is often negligible. The second or nonresonance term in (9) can sometimes even dominate over the first or resonance term, as found in [12] and as illustrated in section 4.2 of the present paper.

It is to be noted here that the width and the height of the Lorentzian profile in (9) or (10) cannot be made independent of each other if the $S$ matrix is required to have a simple pole at $E = E_\mathrm{r} - \mathrm{i}\Gamma/2$ and also to be unitary and symmetric at the same time. The width and the height must be consistent with each other. This fact may be used for error check in numerical calculations.

We have found no simple relation satisfied by the largest eigenvalue $q_\mathrm{max}(E)$ alone, in general. In other words, there seems to be no theoretical guarantee that no other eigenvalues share a part of the whole Lorentzian contribution to $\mathrm{Tr}\, Q(E)$, or that $q_\mathrm{max}(E)$ may be decomposed into the Lorentzian profile and a term with known approximate functional form. In particular, we know of no appropriate fitting formula for $q_\mathrm{max}(E)$ near a threshold in the presence of an overcritical dipole field. On the other hand, the examination of numerical examples from actual applications reveals an outstanding aspect of this eigenvalue; see section 4.2.

A remark is due here on the resonance analysis of photoionization. A resonance formula for the photoionization cross section is sometimes used for fitting to extract resonance parameters. However, there can be many resonances that fail to manifest themselves clearly in the cross section for photoionization of a particular initial bound state. The eigenphase-sum derivative for the final state of photoionization/photodetachment would be much more useful for the purpose of resonance analysis. Much less resonances would be missed in this way than by studying the cross section structure. Also, the fitting can often be numerically more accurate if the eigenphase-sum derivative is used.

## 3. Hyperspherical close-coupling theory

### *3.1. Coupled equations*

The hyperspherical close-coupling (HSCC) method for the system $Ps^-$ is described in some detail in [31], and only a brief explanation suffices here. First, two sets of Jacobi coordinates $(\mathbf{r}_i, \mathbf{R}_i)$ $(i = 1, 2)$ are defined; $\mathbf{r}_i$ is the position vector of the $i$th electron from the positron, and $\mathbf{R}_i$ the relative-distance vector from the centre of mass of the electron–positron pair to the other electron. The hyper-radius $\rho$ for $Ps^-$ is defined by

$$\rho^2 = \tfrac{2}{3}R_i^2 + \tfrac{1}{2}r_i^2, \tag{11}$$

which actually results in the same $\rho$ for both $i = 1$ and 2. All the other five coordinates, denoted collectively by $\Omega$, are angular coordinates called hyperangles, each of which runs

over a finite region. The hyper-radius runs over a semi-infinite region, and it becomes large when any of the three particles lies far from the rest of the system.

The total Hamiltonian is written in the hyperspherical coordinates $(\rho, \Omega)$ as

$$H = -\frac{\hbar^2}{2m_e}\left(\frac{d^2}{d\rho^2} + \frac{5}{\rho}\frac{d}{d\rho}\right) + h_{ad}(\Omega; \rho). \tag{12}$$

Here, $m_e$ is the electron mass and $h_{ad}$ is the part of the Hamiltonian adiabatic in $\rho$ and includes $\rho$ as the adiabatic parameter. The adiabatic channel functions $\{\varphi_i\}$ are defined by

$$h_{ad}(\Omega; \rho)\varphi_i(\Omega; \rho) = U_i(\rho)\varphi_i(\Omega; \rho), \tag{13}$$

where the eigenvalues $\{U_i(\rho)\}$ are the adiabatic potentials. The total wavefunction is expanded as

$$\Psi(\rho, \Omega) = \sum_i \rho^{-5/2} F_i(\rho)\varphi_i(\Omega; \rho) \tag{14}$$

in terms of $\{\varphi_i\}$. Then the radial functions $\{F_i(\rho)\}$ satisfy the HSCC equations

$$\left(-\frac{\hbar^2}{2m_e}\frac{d^2}{d\rho^2} + U_i(\rho) - E\right) F_i(\rho) + \sum_j V_{ij}(\rho)F_j(\rho) = 0 \tag{15}$$

coupled by the nonadiabatic potential $V_{ij}$, which follows from the differential operators in (12). These coupled differential equations are solved up to sufficiently large values of hyper-radius $\rho$, where the wavefunctions are matched to the scattering asymptotic forms in the Jacobi coordinates to extract the reactance matrix, and hence the scattering matrix $S(E)$. The scattering asymptotic forms involve the dipole states explicitly, so that the sometimes crucial effects of the long-range dipole potentials are automatically taken into account up to infinitely large distances.

The time-delay matrix $Q(E)$ has been calculated using (5), in which the $S$ matrix elements have been fitted to cubic spline functions for the purpose of differentiation with respect to the energy $E$. The eigenvalues of the complex $Q(E)$ matrix have been calculated by using the complex QR method.

In the present calculations, we have coupled all the hyperspherical channels associated with the asymptotic limit $e^- + Ps(n)$ with $n = 1$ through 4. This guarantees the convergence of the resonance parameters for those resonances lying near the $Ps(n = 2)$ and $Ps(n = 3)$ thresholds. In some cases the convergence was confirmed by carrying out an elaborate calculation including all channels up to $n = 5$.

One of the advantages of the HSCC method is that nonlocal potentials are completely absent in the scattering equations even though the electron exchange effects are automatically taken account of. This saves much of the computation time compared with solving coupled integro-differential equations in the conventional close-coupling method in the Jacobi coordinates. The HSCC method has proved to be a powerful tool to study resonance states of many three-body systems [39]. The adiabatic hyperspherical potentials already provide transparent visual information on the existence and the mechanisms of resonances, in contrast to the complex-coordinate rotation method, for example. The cross sections and resonance parameters converge rapidly as the number of coupled channels is increased.

### *3.2. Adiabatic potentials and Feshbach resonances*

Resonance states, either Feshbach-type or shape resonances, are normally supported by a particular adiabatic hyperspherical potential curve, or a diabatic potential if there is an avoided crossing between adiabatic potentials. Therefore, they are conveniently assigned in relation to

**Table 1.** The strength $\alpha$ of the asymptotic dipole potential in each $n(K, T)$ channel for partial wave $L$. The channels with a line do not exist since $L < T$ for them.

| $n(K,T)$ | $L=0$ | $L=1$ | $L=2$ | $L=3$ | $L=4$ | $L=5$ |
|---|---|---|---|---|---|---|
| 2(1, 0) | −7.062 | −5.544 | −2.434 | 2.370 | 8.958 | 17.399 |
| 2(0, 1) | — | 2.000 | 6.000 | 12.000 | 20.000 | 30.000 |
| 3(2, 0) | −22.15 | −20.71 | −17.80 | −13.37 | −7.372 | 0.2731 |
| 3(1, 1) | — | −8.166 | −4.945 | 0.000 | 6.743 | 15.34 |
| 3(0, 0) | 3.972 | 5.765 | 4.214 | 10.46 | 18.69 | 28.90 |
| 3(0, 2) | — | — | 9.410 | 14.99 | 22.57 | 32.18 |

the associated channel. The channels or the potential curves are labelled as $^{2S+1}L^{\Pi}n(K, T)^A$ in terms of the total spin ($S$) and orbital ($L$) angular momenta, the parity $\Pi$ and the correlation quantum numbers $K$, $T$ and $A$ after [40, 41].

The quantum number $A$, introduced by Lin, takes a value 0 or $\pm 1$, and is specified by a superscript 0 or $\pm$ [41, 42]. For doubly excited resonance states of He and $H^-$ with $A = \pm 1$, the spectral regularity is characteristic of the rotor-vibrator spectra of linear triatomic molecules, although truncated. The quantum number $T$ is for the projection of the total orbital angular momentum onto the interelectronic axis, and hence, it naturally follows that $T \leqslant L$, provided that $T$ is a fairly good quantum number. An upper limit of $L$, namely,

$$L \leqslant K + n - 1 \tag{16}$$

was found empirically for $H^-$. It was explained for the truncated rotor series, and hence, for $A = \pm$, in terms of shell-model wavefunctions [42].

As was explained just above (3), the asymptotic interaction between a charged particle and an excited neutral hydrogenlike atom is dominated by a dipole potential $\hbar^2\alpha/(2MR^2)$. Analytic expressions for the constant $\alpha$ for the three channels with $n = 2$ are given in [43] for any combination of the masses of the three particles in the system and for any value of $L$. For $Ps^-$, they reduce to formulae

$$\begin{aligned} \alpha_0 &= L(L+1), \\ \alpha_\pm &= L^2 + L + 1 \pm [(2L+1)^2 + 64]^{1/2}. \end{aligned} \tag{17}$$

Some numerical values of $\alpha$ are tabulated in table 1 for channels dissociating asymptotically into $e^- + Ps(n = 2)$ or $e^- + Ps(n = 3)$. They depend on $n$, $K$, $T$ and $L$, but not on $S$, $\Pi$ or $A$.

If $\alpha < -1/4$, the attractive asymptotic dipole potential supports an infinite series of bound states just below the $Ps(n)$ threshold. These bound states turn into Feshbach resonances when coupled with open channels [35]. According to (17), only one of the three potentials (or of the two potentials for the S wave) associated with the $Ps(n = 2)$ threshold, which turns out to be the $n(K, T) = 2(1, 0)$ potential, may have an asymptotically attractive dipole potential. The condition for the existence of an infinite series of Feshbach resonances in $Ps^-$ reads as $(4L^2 + 12L + 9)(4L^2 - 4L + 1) < 32^2$ [43], which is satisfied only by $L = 0$, 1 and 2. This is consistent with table 1, which predicts an infinite series for the partial waves $L = 0$, 1 and 2 with $n(K, T) = 2(1, 0)$. This table predicts an infinite series also for $L = 0$, 1, 2, 3 and 4 with 3(2, 0) and for $L = 1$ and 2 with 3(1, 1). These infinite series for $Ps^-$ are seen to be consistent with the empirical rule (16) found for $H^-$.

The Feshbach series become finite if the sublevel splittings due to the fine structure and the Lamb shift are taken account of. These effects are completely neglected in the present work.

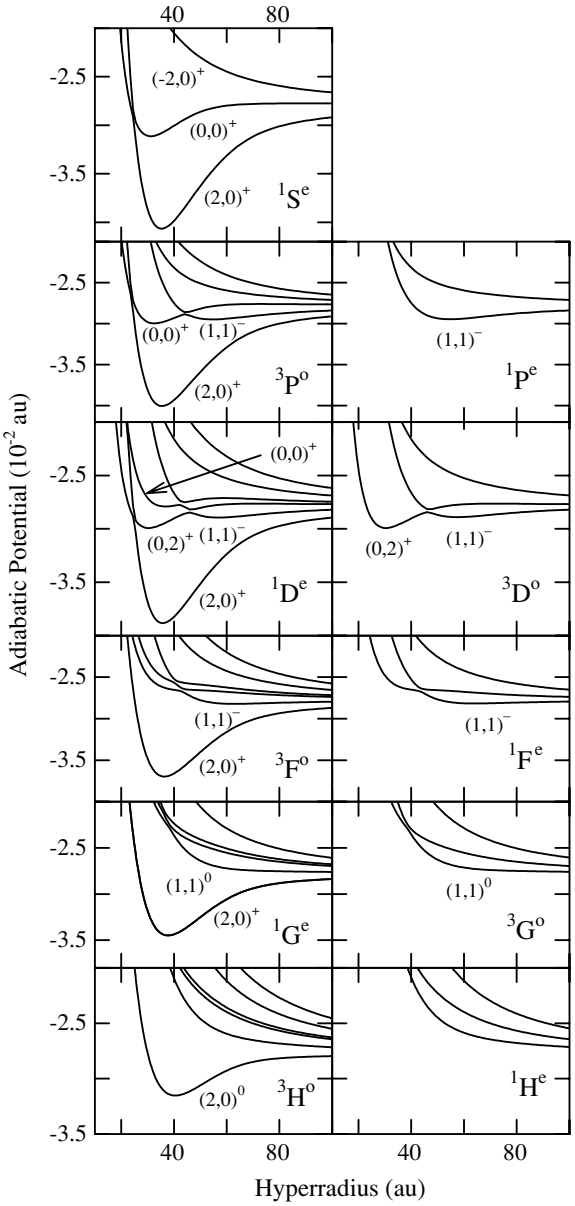


**Figure 1.** Gerade $[\Pi(-1)^S = +1]$ hyperspherical adiabatic potential curves converging asymptotically to the Ps($n = 3$) threshold. (a) Left column: normal parity states $^1S^e$, $^3P^o$, $^1D^e$, $^3F^o$, $^1G^e$ and $^3H^o$. (b) Right column: abnormal parity states $^1P^e$, $^3D^o$, $^1F^e$, $^3G^o$ and $^1H^e$. Each adiabatic potential, or diabatic potential when adiabatic potentials have an avoided crossing, is labelled by the correlation quantum numbers $(K, T)^A$.

Incidentally, there may be a finite number of resonances even for a channel with $\alpha \geqslant -1/4$, if the potential is strongly attractive enough in the inner region.

Figure 1 shows gerade $[\Pi(-1)^S = +1]$ hyperspherical potential curves converging asymptotically to the Ps($n = 3$) threshold, and figure 2 shows ungerade $[\Pi(-1)^S = -1]$

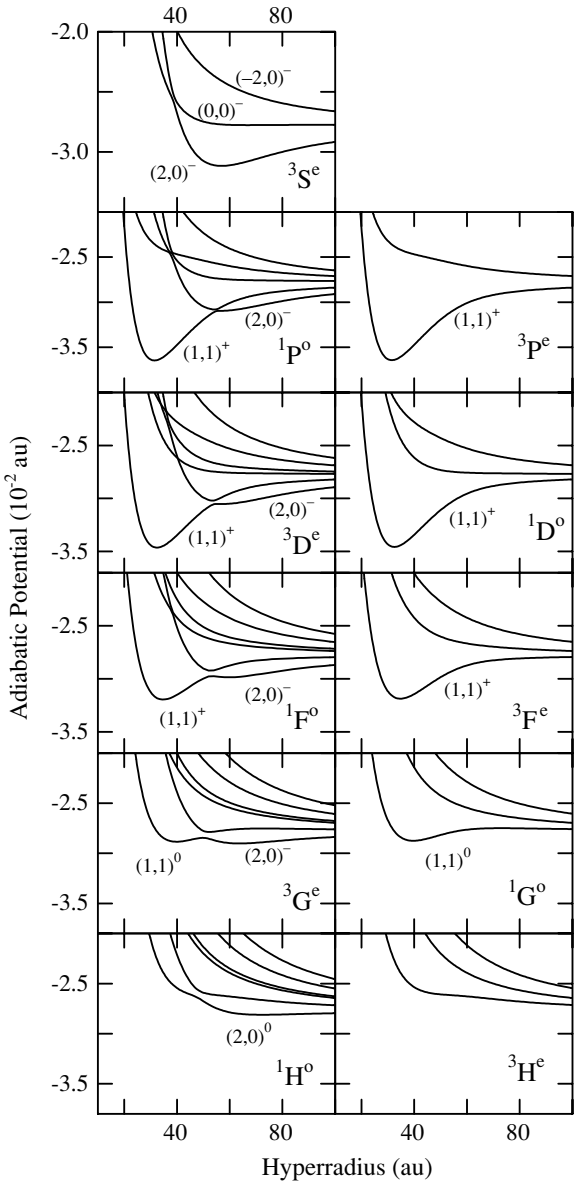


**Figure 2.** Ungerade $[\Pi(-1)^S = -1]$ hyperspherical adiabatic potential curves converging asymptotically to the Ps($n = 3$) threshold. (a) Left column: normal parity states $^3S^e$, $^1P^o$, $^3D^e$, $^1F^o$, $^3G^e$ and $^1H^o$. (b) Right column: abnormal parity states $^3P^e$, $^1D^o$, $^3F^e$, $^1G^o$ and $^3H^e$. See the caption to figure 1 for further explanation.

potentials converging to the same threshold. Those converging to the Ps($n = 2$) threshold are found, for example, in [29, 42]. The adiabatic potentials in figures 1 and 2, or diabatic potentials when avoided crossings occur between adiabatic potentials, are identified by the correlation quantum numbers $(K, T)^A$. The potentials that have common $(K, T)^A$ but different symmetries are seen to be similar and are shifted upwards with the increase of $L$. Therefore, the resonances supported by these potentials are expected to be shifted upwards with the increase

**Table 2.** Energies $E_r$ and widths $\Gamma$ (in au) of $Ps^-$ resonances associated with the Ps($n = 2$) threshold at $E_{th} = -0.0625$ au. The labels for shape resonances are preceded by an asterisk. $x[y] = x \times 10^y$.

| Symmetry | Label | Present HSCC ($E_r$, $\Gamma$) | Complex rotation ($E_r$, $\Gamma$) |
|---|---|---|---|
| $^1S^e$ | $2(1,0)^+$ | $(-7.6029[-2], 4.3[-5])$ | $(-7.6030[-2], 4.3[-5])$[a] |
| | $2(1,0)^+$ | $(-6.3646[-2], 8.6[-6])$ | $(-6.3650[-2], 8.7[-6])$[a] |
| | $2(1,0)^+$ | $(-6.2601[-2], 7.5[-7])$ | $(-6.2601[-2], 1.2[-6])$[a] |
| $^3S^e$ | $2(1,0)^-$ | $(-6.3537[-2], 3.1[-9])$ | $(-6.3530[-2], 5[-6])$[a] |
| $^1P^o$ | $2(1,0)^-$ | $(-6.3155[-2], 9.2[-7])$ | $(-6.3156[-2], 1[-6])$[b] |
| | $2(1,0)^-$ | $(-6.2543[-2], 2.5[-7])$ | |
| | $*2(0,1)^+$ | $(-6.2180[-2], 4.7[-4])$ | $(-6.2170[-2], 4.5[-4])$[b] |
| $^3P^o$ | $2(1,0)^+$ | $(-7.3327[-2], 1.3[-4])$ | $(-7.3327[-2], 1.28[-4])$[b] |
| | $2(1,0)^+$ | $(-6.3095[-2], 1.6[-5])$ | $(-6.3097[-2], 1.6[-5])$[b] |
| | $2(1,0)^+$ | $(-6.2538[-2], 1.0[-6])$ | |
| $^3P^e$ | $*2(0,1)^+$ | $(-6.2199[-2], 2.9[-4])$ | $(-6.2200[-2], 2.7[-4])$[c] |
| $^1D^e$ | $2(1,0)^+$ | $(-6.7911[-2], 1.8[-6])$ | $(-6.7913[-2], 2[-6])$[d] |
| | $2(1,0)^+$ | $(-6.2545[-2], 2.3[-8])$ | |
| $^3D^e$ | $2(1,0)^-$ | $(-6.2588[-2], 2.3[-9])$ | $(-6.2588[-2], 6.4[-6])$[d] |
| $^3F^o$ | $*2(1,0)^0$ | $(-6.2140[-2], 3.7[-4])$ | |

[a] Reference [21].
[b] Reference [22].
[c] Reference [23].
[d] Reference [24].

of $L$. Those potentials that have common $(K, T)^A$ and $L$ but different $S$ and $\Pi$ are quite close to each other. Indeed, every potential in the right column of figure 1 or of figure 2 would be indistinguishable from an adiabatic or a diabatic potential curve in the left column if both columns were brought on top of each other. From this observation follows the expectation that resonances supported by these potentials are almost degenerate in $S$ and $\Pi$ but are shifted upwards with the increase of $L$.

## 4. Results

### *4.1. Resonances near the* Ps($n = 2$) *threshold*

Table 2 summarizes the resonance parameters resulting from the analysis of the present HSCC eigenphase-sum derivative $d\delta/dE$ calculated at energies close to the Ps($n = 2$) threshold. Comparison is made with the results of the complex-coordinate rotation (CCR) calculations by Ho and Bhatia [21–24]. Some members of the infinite series of S-, P- and D-wave $2(1,0)^\pm$-channel Feshbach resonances are found in the table.

Most resonance parameters agree well between the present HSCC calculations and the CCR calculations; the only exceptions are the $2(1,0)^-$ resonances of $^3S^e$ and $^3D^e$ symmetries, for which the present widths of $3 \times 10^{-9}$ au and $2 \times 10^{-9}$ au are seen to be much narrower than the CCR widths of $5 \times 10^{-6}$ au [21] and $6 \times 10^{-6}$ au [24]. The reason for this disagreement is still unknown. The $^3S^e$ widths of $3 \times 10^{-9}$ au by Papp *et al* [33] and $2 \times 10^{-9}$ au by Suzuki and Usukura [34] happen to be closer to the present results.

A shape resonance supported by the $^3F^o 2(1,0)^0$ potential is found just above the Ps($n = 2$) threshold, perhaps for the first time. This resonance violates the empirical rule (16) for $H^-$, although it may not be too surprising since it is an $A = 0$ resonance; no resonance in $H^-$ with

$L \geqslant 3$ have been found close to the H($n = 2$) threshold, anyway, as far as we are aware. For $Ps^-$ the present calculations detect no resonances beyond $L = 3$ near the Ps($n = 2$) threshold.

$Ps^-$ shape resonances are also seen in the $2(0, 1)^+$ channels of symmetries $^1P^o$ and $^3P^e$. The latter resonance corresponds to the bound state of $H^-(^3P^e)$, which is pushed up for $Ps^-$ to above the $n = 2$ threshold due to the mass effect [29, 42].

### *4.2. Resonances near the* Ps($n = 3$) *threshold*

The resonance parameters extracted from the eigenphase-sum derivative near the Ps($n = 3$) threshold are summarized in table 3 for gerade states and in table 4 for ungerade states. Among these resonances, some belong to the $3(2, 0)^{\pm}$ infinite series of Feshbach resonances with $L = 0 - 4$ and others to the $3(1, 1)^{\pm}$ infinite series with $L = 1$ and 2. Tables 3 and 4 also include many other Feshbach and shape resonances, which are independent of any infinite series.

It has been noted at the end of section 3.2 that potentials in figures 1 and 2 having common $(K, T)^A$ and $L$ but different $S$ and $\Pi$ are practically indistinguishable from each other, probably resulting in pairs of resonances almost degenerate in $S$ and $\Pi$. Indeed, such almost degenerate pairs are found; P $3(1, 1)^-$, D $3(1, 1)^-$ and D $3(0, 2)^+$ gerade pairs of resonances in table 3, and three P $3(1, 1)^+$ pairs, two D $3(1, 1)^+$ pairs and one F $3(1, 1)^+$ pair of ungerade resonances in table 4.

The resonance parameters in tables 3 and 4 are generally in good agreement with those of the CCR method, except for the $^1S^e$ $3(0, 0)^+$ resonance and the second $^3D^e$ $3(2, 0)^-$ resonance, for which the HSCC widths are narrower than the CCR values by nearly an order of magnitude.

The $^1S^e$ $3(0, 0)^+$ and $^1D^e$ $3(0, 2)^+$ shape resonances correspond to Feshbach resonances in $H^-$ below the H($n = 3$) threshold. These $H^-$ resonances are pushed up for $Ps^-$ to above the $n = 3$ threshold due to the mass effect [26, 42].

The $^3H^o$ $3(2, 0)^0$ ($L = 5$) Feshbach resonance, found here for the first time for $Ps^-$, violates the empirical rule (16) for $H^-$. It is an $A = 0$ resonance just as the $Ps^-$ $^3F^o$ $2(1, 0)^0$ shape resonance violating (16). No $H^-$ resonances beyond $L = 4$ and near the H($n = 3$) threshold seems to have been reported in the literature. The increase in the number of resonances in $Ps^-$ compared with $H^-$ clearly reflects the fact that $Ps^-$ lies intermediate between the atomic limit $H^-$ and the molecular limit $H_2^+$.

A group of shape resonances of symmetries $^1S^e$, $^3P^o$ and $^1D^e$ in table 3 deserves special attention. The CCR method predicted these resonances, but the HSCC eigenphase sum $\delta(E)$ fails to show a typical full-resonance structure; see figure 3. The $^1S^e$ eigenphase sum increases rapidly, as in a typical resonance, although only by a little more than 1 rad. For $^3P^o$ and $^1D^e$, the eigenphase sum $\delta(E)$ decreases monotonically, indicating a negative average delay time or that the average collision time is shorter than in the absence of the projectile–target interaction. This is evidently due to the extremely strong effects of the background eigenphase sum $\delta^0(E)$ as discussed in section 2, namely, due to the logarithmically diverging $\delta^0(E)$ as $E$ approaches the threshold for Ps($n = 3$) from above in the presence of the overcritical dipole potential created by the linear Stark effect on the degenerate sublevels of Ps($n = 3$). The highly negative slope of $\delta^0(E)$ invokes the need of using (4) or (10) in the fitting procedure, instead of (2). The threshold effect seems to be weaker for $^1S^e$ in the energy region of this shape resonance. Incidentally, another case of the effects of an $S$-matrix pole being washed away by a strong background was illustrated previously in analysing the system $e^+He^+$ [12].

Also included in figure 3 are the eigenvalues $\{q_i(E)\}$ (full curves) of the time-delay matrix $Q(E)$ and their sum, i.e. Tr $Q(E)$ (dashed curves). For $^1S^e$, Tr $Q(E)$ and the largest eigenvalue $q_{\max}(E)$ exhibit quite similar energy dependence, one being almost a mere vertical shift of the

**Table 3.** Energies $E_r$ and widths $\Gamma$ (in au) of gerade $[\Pi(-1)^S = +1]$ resonances in $Ps^-$ associated with the $Ps(n = 3)$ threshold at $E_{th} = -0.02778$ au. The labels for shape resonances are preceded by an asterisk. $x[y] = x \times 10^y$.

| Symmetry | Label | Present HSCC ($E_r$, $\Gamma$) | Complex rotation ($E_r$, $\Gamma$) |
|---|---|---|---|
| $^1S^e$ | $3(2,0)^+$ | $(-3.5338[-2], 7.6[-5])$ | $(-3.5342[-2], 7.47[-5])^a$ |
| | | | $(-3.5342[-2], 7.44[-5])^b$ |
| | $3(2,0)^+$ | $(-2.9841[-2], 5.3[-5])$ | $(-2.9846[-2], 5.27[-5])^a$ |
| | | | $(-2.9846[-2], 5.25[-5])^b$ |
| | $3(2,0)^+$ | $(-2.8287[-2], 1.2[-5])$ | $(-2.8296[-2], 1.15[-5])^b$ |
| | $3(2,0)^+$ | $(-2.7909[-2], 3.4[-6])$ | |
| | $*3(0,0)^+$ | $(-2.7741[-2], 6.8[-6])$ | $(-2.7725[-2], 4.2[-5])^a$ |
| $^3P^o$ | $3(2,0)^+$ | $(-3.4868[-2], 6.1[-5])$ | $(-3.4872[-2], 6.08[-5])^b$ |
| | | | $(-3.4871[-2], 6.06[-5])^c$ |
| | $3(2,0)^+$ | $(-2.9594[-2], 4.2[-5])$ | $(-2.9600[-2], 4.21[-5])^b$ |
| | | | $(-2.9600[-2], 4.11[-5])^c$ |
| | $3(2,0)^+$ | $(-2.8233[-2], 4.9[-6])$ | |
| | $3(1,1)^-$ | $(-2.8182[-2], 4.5[-6])$ | |
| | $3(2,0)^+$ | $(-2.7883[-2], 2.4[-6])$ | |
| | $*3(0,0)^+$ | $(-2.7249[-2], 4.8[-4])$ | $(-2.725[-2], 4.60[-4])^c$ |
| $^1P^e$ | $3(1,1)^-$ | $(-2.8201[-2], 8.2[-9])$ | |
| $^1D^e$ | $3(2,0)^+$ | $(-3.3911[-2], 2.4[-5])$ | $(-3.3914[-2], 2.28[-5])^b$ |
| | | | $(-3.3914[-2], 2.36[-5])^d$ |
| | $3(2,0)^+$ | $(-2.9121[-2], 1.5[-5])$ | $(-2.9125[-2], 1.35[-5])^b$ |
| | | | $(-2.9127[-2], 1.40[-5])^d$ |
| | $3(2,0)^+$ | $(-2.8071[-2], 2.5[-6])$ | |
| | $3(1,1)^-$ | $(-2.7951[-2], 9.4[-7])$ | |
| | $3(2,0)^+$ | $(-2.7840[-2], 7.5[-7])$ | |
| | $*3(0,2)^+$ | $(-2.7480[-2], 3.1[-4])$ | $(-2.7400[-2], 3.2[-4])^d$ |
| | $*3(0,0)^+$ | $(-2.617[-2], 2.1[-3])$ | $(-2.618[-2], 2.04[-3])^c$ |
| $^3D^o$ | $3(1,1)^-$ | $(-2.7947[-2], 7.1[-7])$ | $(-2.7949[-2], < 1.5[-6])^e$ |
| | $*3(0,2)^+$ | $(-2.7480[-2], 3.2[-4])$ | $(-2.7485[-2], 3.10[-4])^e$ |
| $^3F^o$ | $3(2,0)^+$ | $(-3.2473[-2], 8.5[-5])$ | $(-3.2475[-2], 8.29[-5])^b$ |
| | $3(2,0)^+$ | $(-2.8503[-2], 2.9[-5])$ | |
| | $3(2,0)^+$ | $(-2.7902[-2], 5.1[-6])$ | |
| | $3(2,0)^+$ | $(-2.7800[-2], 9.7[-7])$ | |
| $^1G^e$ | $3(2,0)^+$ | $(-3.0673[-2], 8.2[-5])$ | $(-3.0682[-2], 8.25[-5])^b$ |
| | $3(2,0)^+$ | $(-2.7968[-2], 9.6[-6])$ | |
| $^3H^o$ | $3(2,0)^0$ | $(-2.8569[-2], 4.5[-6])$ | $(-2.8577[-2], 3.0[-6])^b$ |

[a] Reference [21].
[b] Reference [28].
[c] Reference [22].
[d] Reference [24].
[e] Reference [25].

other. For $^3P^o$ and $^1D^e$ having much stronger background effects, $q_{max}(E)$ is found to have a much clearer Lorentzian-like profile than Tr $Q(E)$. In particular, the broader of the two $^1D^e$ shape resonances, which is evident in $q_{max}(E)$, is hardly discernible in the dashed curve of Tr $Q(E)$. The eigenvalues $\{q_i(E)\}$ in figures 3(b) and (c) other than $q_{max}(E)$ are either close to zero or negative and large, making the whole sum, Tr $Q(E)$, negative and of a complicated profile. The diverging background eigenphase sum appears to be nearly fully accommodated by the eigenvalues $\{q_i(E)\}$ other than the largest; any strong background effects are hardly

**Table 4.** Energies $E_r$ and widths $\Gamma$ (in au) of ungerade $[\Pi(-1)^S = -1]$ resonances in $Ps^-$ associated with the $Ps(n = 3)$ threshold at $E_{th} = -0.02778$ au. All resonances in this table are Feshbach resonances. $x[y] = x \times 10^y$.

| Symmetry | Label | Present HSCC[a] ($E_r$, $\Gamma$) | Complex rotation ($E_r$, $\Gamma$) |
|---|---|---|---|
| $^3S^e$ | $3(2,0)^-$ | $(-2.9368[-2], 2.1[-7])$ | $(-2.9371[-2], 1.85[-7])$[c] |
| | $3(2,0)^-$ | $(-2.8183[-2], 8.1[-8])$ | |
| | $3(2,0)^-$ | $(-2.7883[-2], 2.3[-8])$ | |
| $^1P^o$ | $3(1,1)^+$ | $(-3.1621[-2], 2.2[-4])$[b] | $(-3.1622[-2], 2.21[-4])$[d] |
| | $3(2,0)^-$ | $(-2.9212[-2], 1.5[-6])$[b] | $(-2.9215[-2], 1.5[-6])$[d] |
| | $3(2,0)^-$ | $(-2.8125[-2], 6.0[-7])$[b] | |
| | $3(1,1)^+$ | $(-2.8099[-2], 3.3[-5])$[b] | |
| | $3(2,0)^-$ | $(-2.7864[-2], 8.7[-8])$[b] | |
| | $3(1,1)^+$ | $(-2.7811[-2], 3.5[-6])$[b] | |
| $^3P^e$ | $3(1,1)^+$ | $(-3.1626[-2], 1.8[-4])$ | $(-3.1631[-2], 1.80[-4])$[c] |
| | | | $(-3.1631[-2], 1.79[-4])$[e] |
| | $3(1,1)^+$ | $(-2.8100[-2], 2.7[-5])$ | $(-2.8105[-2], 2.74[-5])$[e] |
| | $3(1,1)^+$ | $(-2.7811[-2], 2.9[-6])$ | |
| $^3D^e$ | $3(1,1)^+$ | $(-3.0410[-2], 1.3[-4])$ | $(-3.0410[-2], 1.31[-4])$[c] |
| | | | $(-3.0411[-2], 1.32[-4])$[f] |
| | $3(2,0)^-$ | $(-2.8906[-2], 2.9[-6])$ | $(-2.8907[-2], 4.2[-6])$[f] |
| | $3(2,0)^-$ | $(-2.8021[-2], 3.6[-7])$ | $(-2.8021[-2], 3.2[-6])$[f] |
| | $3(1,1)^+$ | $(-2.7874[-2], 7.6[-6])$ | |
| | $3(2,0)^-$ | $(-2.7832[-2], 1.2[-7])$ | |
| $^1D^o$ | $3(1,1)^+$ | $(-3.0434[-2], 7.3[-5])$ | $(-3.0441[-2], 7.2[-5])$[c] |
| | | | $(-3.0441[-2], 7.20[-5])$[g] |
| | $3(1,1)^+$ | $(-2.7876[-2], 4.5[-6])$ | |
| $^1F^o$ | $3(1,1)^+$ | $(-2.8695[-2], 4.0[-5])$ | $(-2.8700[-2], 5.52[-5])$[c] |
| | $3(2,0)^-$ | $(-2.8377[-2], 2.7[-5])$ | |
| | $3(2,0)^-$ | $(-2.7893[-2], 6.1[-7])$ | |
| $^3F^e$ | $3(1,1)^+$ | $(-2.8599[-2], 1.1[-5])$ | $(-2.8611[-2], 1.01[-5])$[c] |
| $^3G^e$ | $3(2,0)^-$ | $(-2.8046[-2], 4.4[-7])$ | |

[a] Present results except for those with a superscript b.
[b] Reference [31].
[c] Reference [28].
[d] Reference [22].
[e] Reference [23].
[f] Reference [24].
[g] Reference [25].

observable in $q_{max}(E)$. This should be possible to explain in some way or other, although such a theory remains to be developed. In spite of the lack of theoretical justification when the background $S$ matrix depends strongly on the energy, an attempt has been made to fit the right-hand side of (10) without the diverging term to the numerical values of $q_{max}(E)$. This has produced practically the same resonance parameters as obtained from the Tr $Q(E)$ fitting, which is certainly instructive.

The $^1D^e$ partial-wave cross sections $\sigma(3s \rightarrow 3l)$ for sublevel transitions are shown in figure 4. The structure in each curve looks quite typical of the so-called dipole oscillation phenomenon caused by the overcritical dipole field [35, 36]. Taking the largest negative $\alpha$ value ($= -17.8$) for the D wave from table 1 and consulting (3), one may estimate the ratio between the energy positions of two adjacent peaks or dips in the dipole oscillation to be

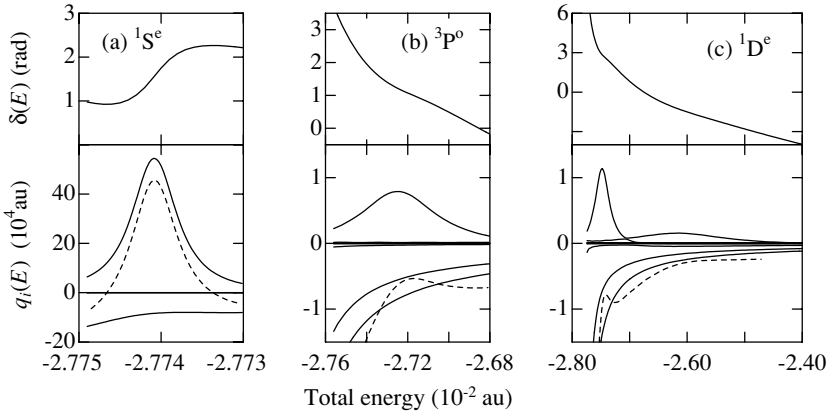


**Figure 3.** The eigenphase sum $\delta(E)$ and the trace $(= 2\hbar \mathrm{d}\delta/\mathrm{d}E)$ (- - - -) and the eigenvalues $\{q_i(E)\}$ (——) of the time-delay matrix $Q(E)$ plotted against the total energy $E$ above the Ps($n = 3$) threshold $E_{\mathrm{th}}$ ($= -0.02778$ au). (a) $^1$S$^e$. (b) $^3$P$^o$. (c) $^1$D$^e$. The number of open channels is 6 for (a), 9 for (b) and 10 for (c). Some $q_i(E)$ are too small to be distinguished from the zero line.

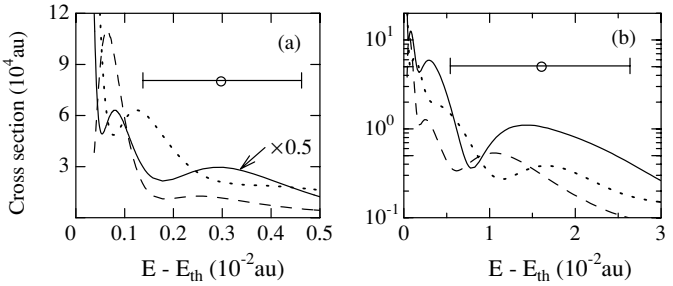


**Figure 4.** The $^1$D$^e$ partial-wave cross sections in $e^-$ + Ps(3s) scattering for (a) $0 < E - E_{\mathrm{th}} < 5 \times 10^{-3}$ au and (b) $0 < E - E_{\mathrm{th}} < 3 \times 10^{-2}$ au, where $E$ is the total energy and $E_{\mathrm{th}}$ is the Ps($n = 3$) threshold. ——: 3s → 3s. – – –: 3s → 3p. · · · · · ·: 3s → 3d. The resonance positions and widths are indicated by circles and bars.

about 4.5. Roughly speaking, this is consistent with the structure in figure 4. Therefore, this structure may be understood to be due mainly to the dipole oscillation, which is repeated infinite times towards the threshold. The structure is slightly modified by the *S*-matrix poles, of which the positions and widths are indicated by circles and horizontal lines in figure 4. The P-wave cross section, not shown here, also exhibits what may be interpreted as dipole oscillation, naturally at energy positions different from the D wave since the strength of the dipole potential is different.

### *4.3. Cross sections for* $e^-$ + Ps(1s) *scattering*

Resonance structures in the total cross sections are less conspicuous in general than those in partial-wave cross sections. Nevertheless, the spin-weighted and partial-wave summed elastic cross section for $e^-$ + Ps(1s) scattering still shows a rich structure at energies just below the Ps($n = 2$) threshold, as seen in figure 5. There, the partial-wave cross sections are summed up to $L = 5$, which is sufficient in the energy region of figure 5. For the initial state Ps(1s), only the symmetries with $\Pi = (-1)^L$ contribute to the cross section.

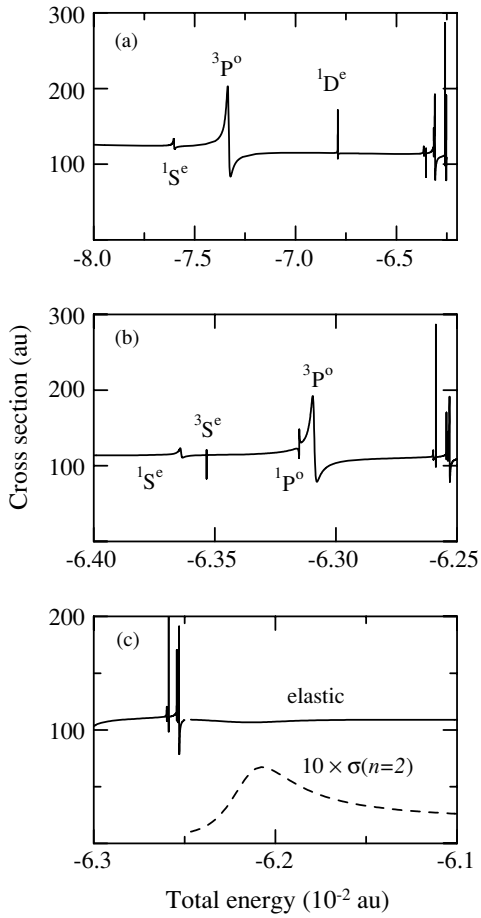


**Figure 5.** Spin-weighted cross sections for $e^- + Ps(1s)$ scattering for total energy $E$ (in au) around the $Ps(n = 2)$ threshold ($E_{th} = -0.0625$ au). ——: elastic. – – –: excitation into $Ps(n = 2)$. (a) $-0.08 < E < -0.062$. (b) $-0.064 < E < -0.0625$. (c) $-0.063 < E < -0.061$.

The lowest $^3P^o$ resonance at $E = -7.333 \times 10^{-2}$ au has the largest width of $1.3 \times 10^{-4}$ au and affects the cross section most strongly in the energy region of figure 5. Above the threshold $E_{th}(n = 2) = -0.0625$ au the elastic cross section in figure 5(c) is nearly flat, but the cross section for excitation into $Ps(n = 2)$ shows a peak with a width of $\sim 5 \times 10^{-4}$ au ($\simeq 0.015$ eV) because of the two shape resonances of symmetries $^1P^o$ and $^3F^o$ at $E \sim -0.0622$ au. Even at the maximum the excitation cross section is smaller than the elastic cross section by a factor of 15.

The calculations are extended into lower energies than shown in figure 5. An overall agreement is found with the elastic cross section calculated by Ward *et al* [44] at those lower energies where the cross section is smooth as a function of the energy.

## 5. Summary

We have discussed a theory of resonance analysis in scattering and photoionization/ photodetachment. This theory has the advantage of both practical convenience and physical

significance even when the background effects are quite strong. We have exploited the knowledge of properties of the time-delay matrix $Q(E)$, the fact that the eigenphase-sum derivative has a significance of average time delay in the process regardless of the strength of the background effects, and the logarithmic divergence of the eigenphase sum towards a threshold of a new channel in the presence of an overcritical dipole potential.

As an application, we have analysed the results of extensive hyperspherical close-coupling calculations of the system $Ps^-$, and obtained positions and widths of many resonances of partial waves $L \leqslant 5$ close to the thresholds of Ps($n = 2, 3$). The resonance parameters have been compared with the values in the literature, if any. In particular, careful comparison has been made with the complex-coordinate rotation calculations by Ho and collaborators. The agreement is quite good except for a few cases where the widths are in disagreement. Some of the resonances have been found for the first time in the present work. They include those of high partial waves such as $^3F^o\,2(1,0)^0$ and $^3H^o\,3(2,0)^0$ resonances, for which no corresponding resonances are reported in the literature for a similar system $H^-$.

The $^3P^o$ and $^1D^e$ shape resonances above the Ps($n = 3$) threshold, found previously in complex-coordinate rotation calculations, are missing in the eigenphase sum $\delta(E)$ calculated in the present work in the sense that $\delta(E)$ is a monotonically decreasing function of $E$ in the relevant energy region. This means that the electron–positronium collision in this energy region has a negative average time delay in spite of the presence of the $S$-matrix poles predicted by the complex-coordinate calculations. The analysis in terms of the trace of the time-delay matrix or, equivalently, in terms of the eigenphase-sum derivative has clearly singled out the effects of the $S$-matrix poles from the extremely strong background effects that are due to the overcritical dipole field resulting from the linear Stark effect. The largest eigenvalue of the time-delay matrix is found to extract the Lorentzian profile with hardly any background, the profile that is typical of a resonance. This is still to be theoretically explained for the case where the background $S$ matrix has a strong energy dependence. The P- and D-wave cross sections for subshell transitions Ps($3s \rightarrow 3l$) are found to show a distinct threshold oscillatory structure due to the overcritical dipole field.

## Acknowledgments

This work was supported in part by the Ministry of Education, Science, Sports and Technology, Japan and the collaborative programme of the National Institute for Fusion Science, Japan (AI).

## References

[1] See, for example, Blatt J M and Weisskopf V F 1979 *Theoretical Nuclear Physics* (New York: Springer) chapter 10
[2] Hazi A U 1979 *Phys. Rev.* A **19** 920
[3] Tennyson J and Noble C J 1984 *Comput. Phys. Commun.* **33** 421
[4] Smith F T 1960 *Phys. Rev.* **118** 349
[5] Celenza L and Tobocman W 1968 *Phys. Rev.* **174** 1115
[6] Burke P G, Cooper J W and Ormonde S 1969 *Phys. Rev.* **183** 245
[7] Stibbe D T and Tennyson J 1996 *J. Phys. B: At. Mol. Opt. Phys.* **29** 4267
[8] Quigley L and Berrington K 1996 *J. Phys. B: At. Mol. Opt. Phys.* **29** 4529
[9] Ballance C P, McLaughlin B M, Nagy O, Berrington K A and Burke P G 1998 *J. Phys. B: At. Mol. Opt. Phys.* **31** L305
[10] Ballance C P, Berrington K A and McLaughlin B M 1999 *Phys. Rev.* A **60** R4217
[11] Forrey R C, Balakrishnan N, Kharchenko V and Dalgarno A 1998 *Phys. Rev.* A **58** R2645
[12] Igarashi A and Shimamura I 2004 *Phys. Rev.* A **70** 012706

[13] Mills A P Jr 1981 *Phys. Rev. Lett.* **46** 717
[14] Mills A P Jr 1983 *Phys. Rev. Lett.* **50** 671
[15] Schwalm D, Fleischer F, Lestinsky M, Degreif K, Gwinner G, Liechtenstein V, Plenge F and Scheit H 2004 *Nucl. Instrum. Methods* B **221** 185
[16] Balling P, Fregenal D, Ichioka T, Knudsen H, Kristiansen H-P E, Merrison J and Uggerhøj U I 2004 *Nucl. Instrum. Methods* B **221** 200
[17] Ho Y K 1993 *Phys. Rev.* A **48** 4780
[18] Korobov V I 2000 *Phys. Rev.* A **61** 064503
[19] Drake G W F, Cassar M M and Nistor R A 2002 *Phys. Rev.* A **65** 054501
[20] Frolov A M and Smith V H Jr 2003 *J. Phys. B: At. Mol. Opt. Phys.* **36** 4837
[21] Ho Y K 1979 *Phys. Rev.* A **19** 2347
Ho Y K 1984 *Phys. Lett.* A **102** 348
[22] Bhatia A K and Ho Y K 1990 *Phys. Rev.* A **42** 1119
Ho Y K and Bhatia A K 1991 *Phys. Rev.* A **44** 2890
Ho Y K and Bhatia A K 1993 *Phys. Rev.* A **47** 1497
[23] Ho Y K and Bhatia A K 1992 *Phys. Rev.* A **45** 6268
[24] Bhatia A K and Ho Y K 1993 *Phys. Rev.* A **48** 264
[25] Ho Y K and Bhatia A K 1994 *Phys. Rev.* A **50** 2155
[26] Ho Y K 1994 *Hyp. Int.* **89** 401
[27] Ho Y K 1997 *Chin. J. Phys. (Taipei)* **35** 97
[28] Ivanov I and Ho Y K 1999 *Phys. Rev.* A **60** 1015
Ivanov I and Ho Y K 2000 *Phys. Rev.* A **61** 032501
[29] Botero J and Greene C H 1985 *Phys. Rev.* A **32** 1249
Botero J and Greene C H 1986 *Phys. Rev. Lett.* **56** 1366
Botero J 1987 *Phys. Rev.* A **35** 36
[30] Zhou Y and Lin C D 1995 *Phys. Rev. Lett.* **75** 2296
[31] Igarashi A, Shimamura I and Toshima N 2000 *New J. Phys.* **2** 17
[32] Toyota K and Watanabe S 2003 *Phys. Rev.* A **68** 062504
[33] Papp Z, Darai J, Nishimura A, Hlousek Z T, Hu C-Y and Yakovlev S L 2002 *Phys. Lett.* A **304** 36
[34] Suzuki Y and Usukura J 2004 *Nucl. Instrum. Methods* B **221** 195
[35] Gailitis M and Damburg R 1963 *Proc. Phys. Soc.* **82** 192
[36] Greene C, Fano U and Strinati G 1979 *Phys. Rev.* A **19** 1485
[37] Clark C W 1984 *Phys. Rev.* A **30** 750
[38] Callaway J 1981 *Phys. Lett.* A **81** 495
[39] Lin C D 1995 *Phys. Rep.* **257** 1
[40] Herrick D R and Sinanoglu O 1975 *Phys. Rev.* A **11** 97
Herrick D R 1975 *Phys. Rev.* A **12** 413
[41] Lin C D 1986 *Adv. At. Mol. Phys.* **22** 77
[42] Chen Z and Lin C D 1990 *Phys. Rev.* A **42** 18
[43] Shimamura I 1989 *Phys. Rev.* A **40** 4863
[44] Ward S J, Humberston J W and McDowell M R C 1987 *J. Phys. B: At. Mol. Phys.* **20** 127